In situ analysis of plasticity and damage nucleation in a Ti-6Al-4V alloy and laser weld

Cyril Lavogiez[1], Sylvain Dancette[*], Sophie Cazottes, Christophe Le Bourlot, Eric Maire

Univ Lyon, INSA Lyon, CNRS UMR5510, Laboratoire MATEIS, F-69621 Villeurbanne Cedex, France

A B S T R A C T

The present work addresses the mechanisms of plasticity and damage nucleation in a Ti-6Al-4V alloy and its laser weld. To this end, in situ tensile tests are performed in a Scanning Electron Microscope (SEM) equipped with a Electron BackScatter Diffraction (EBSD) camera. The slip activity is automatically analyzed using a modified Schmid analysis. It is shown that the slip activity of the base metal consists mainly in prismatic, basal and pyramidal $\langle a \rangle$ slip. Damage nucleation in the vicinity of the β phase and at α grain boundaries is also evidenced in the base metal. In the α' weld metal (a microstructure similar to the one often obtained in additive manufacturing Ti-alloy parts), plastic deformation results in a crystallographic rotation of the laths tending to align the $\langle 10\bar{1}0 \rangle$ direction with the tensile axis. The rare events of crack initiation in the martensite are shown to occur along specific laths interfaces, former β grain boundary or twinned martensite needles.

1. Introduction

Ti-6Al-4V is the most widely used titanium alloy in the industry accounting for nearly 50% in tonnage of the Ti alloys production. It shows good mechanical properties up to temperatures as high as 400 °C for a light weight – around 60% of the steel density [1]. This explains why the aeronautic industry consumes the majority of the Ti-6Al-4V production. Other remarkable properties are a good corrosion resistance and biocompatibility allowing this alloy to be used in the chemical or biomedical industry as well.

In structural applications, Ti-6Al-4V components can be joined by laser beam welding. This process induces a high cooling rate in the fusion zone (FZ) leading to an α' martensitic microstructure [2]. In the heat affected zone (HAZ) a microstructural gradient is found between the martensitic phase of the FZ and the dual phase microstructure of the base metal. The resulting microstructure is hence composed of the α, β and α' phases [2]. Ti-6Al-4V alloys with good ductile properties generally show two types of microstructure: bimodal or globular equiaxed. Both are obtained from the same processing route, but differ during the recrystallization step. If the corresponding temperature or cooling rate of this step is sufficiently low, then a globular equiaxed microstructure is obtained [3]. Otherwise, the bimodal microstructure is obtained with the presence of secondary α lamellas and primary α nodules.

The nucleation of voids within Ti-6Al-4V alloys is observed in the vicinity of α/β interfaces or specific α grain boundaries [5,6]. Such microstructural heterogeneities can have a strong influence on the plastic behavior of the alloy. For instance, α/β interfaces act as α glide system filters and facilitate basal slip activation in the α lamella colonies [7]. Nevertheless, the crystallographic orientation of α nodules and colonies regarding to the loading direction is the first order parameter to determine which slip system will be activated during plastic deformation [8]. The common slip systems of α titanium are recalled in Table 1. Based upon the Schmid analysis, if the angle between the $\langle c \rangle$ axis of the unit cell and the tensile direction is $> 45°$ then the prismatic slip is activated. If this angle is $< 45°$, then the basal slip is activated. In all cases, pyramidal slip systems are less likely to be activated [4,9] and twinning does not constitute a favorable deformation mode in uniaxial tension.

In the case of the α' martensite microstructure, microstructural heterogeneities consist in the crystallographic orientation of the needles, their morphological orientation and the location of the prior β grain boundaries. In addition to dislocation slip, studies on the deformation behavior of martensite reported the occurrence of $\{10\bar{1}1\}$ twinning [10,11]. The plastic behavior of α' needles also depends on their crystallographic orientations. Under monotonic tension, damage nucleation in martensitic microstructures has been observed at the needle interfaces [12] and at the prior β grain boundaries [13,14].

It is therefore of great interest to investigate the ductile damage of

Table 1
Slip systems in α titanium alloys. Critical Resolved Shear Stress (CRSS) in MPa.

Slip mode	Slip systems	CRSS (Bridier et al. [4])
Basal	$\{0001\}\langle 2\bar{1}\bar{1}0\rangle$	420
Prismatic	$\{0\bar{1}10\}\langle 2\bar{1}\bar{1}0\rangle$	370
Pyramidal I $\langle a\rangle$	$\{0\bar{1}11\}\langle 2110\rangle$	490
Pyramidal I $\langle c + a\rangle$	$\{0\bar{1}11\}\langle 11\bar{2}3\rangle$	590
Pyramidal II $\langle c + a\rangle$	$\{2\bar{1}\bar{1}2\}\langle \bar{2}113\rangle$	590

Ti-6Al-4V in relation with plasticity and microstructure. The present paper presents a multiscale analysis combining Scanning Electron Microscope (SEM) in situ tensile tests with Electron BackScatter Diffraction (EBSD), performed on a Ti-6Al-4V alloy and its laser weld. The work aims at better understanding the mechanisms leading to heterogeneous plastic flow up to the initiation of damage. The experimental procedure is firstly presented, followed by detailed observations of plasticity in the base metal and the weld and their consequences on damage development as observed in situ.

2. Materials and Methods

The studied samples are part of Ti-6Al-4V made structures. The chemical composition of the alloy is detailed in Table 2. They were collected by electro-erosion from two different annealed tubes: one made of a single piece and another one made from two pieces joined by Nd:YAG pulsed laser beam welding along their perimeter.

The base metal (BM) tensile sample geometry is displayed in Fig. 1-a. It was cut along the longitudinal direction of the tube. The microstructure of the BM sample is equiaxed as can be seen on the optical micrograph shown in Fig. 2-a, obtained after mechanical polishing followed by etching in a $C_2H_2O_4 + HF + H_2O$ solution. Globular hexagonal close compact α grains (lattice parameters $a = 0.295$ nm; $c = 0.473$ nm) are surrounded by thin layers of body centered cubic β phase (lattice parameter $a = 0.320$ nm).

The welded tensile sample presents the particular geometry shown in Fig. 1-b and was cut perpendicular to the laser weld line. The small size of the weld bead required two cross-section reductions to localize the plastic flow in the FZ. A metallographic cross-section in the weld is shown in Fig. 2-b, with a zoom on the transition between the BM, HAZ and fusion zone microstructures in Fig. 2-c. The microstructure of the fusion zone is composed of acicular α' martensite needles. Such microstructure is commonly observed in the fusion zone or upper HAZ of titanium alloys subjected to laser welding due to the high cooling rates from the β domain experienced during the process [15,16]. The Vickers microhardness profiles (500 g load) depicted in Fig. 2-d illustrate a slight increase in hardness from the BM ($\sim 330HV_{0.5}$) to the FZ ($\sim 360HV_{0.5}$), with a local maximum in the HAZ where grain refinement occurred as seen in Fig. 2-c.

The two tensile samples tested in situ were mechanically polished using diamond paste down to 3 and 1 µm, followed by vibratory polishing for 2 h using a Struers OPS solution. The in situ experiments were performed on a ZEISS Supra 55VP SEM equipped with an Oxford Instrument Nordlys EBSD camera. Tensile tests were carried out on a commercial GATAN DEBEN 2000E tensile stage designed to fit in the SEM chamber, with a loading rate of 0.1 mm/min. Macroscopic plastic strain was computed from the imposed displacement. As the machine stiffness of the tensile stage is rather low, the computed total
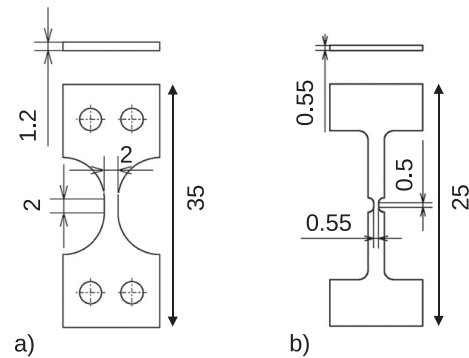
Fig. 1. Geometry of a) base metal sample and b) weld sample (mm).

(elastic + plastic) strain cannot be transposed to macroscopic tensile tests. Plastic strain values only (ε_p) will therefore be discussed in the following. The tensile direction corresponds to the X direction of the EBSD maps (longitudinal tube direction), Z direction being normal to the observation surface. X direction Inverse Pole Figure maps (IPF X maps) will later be referred to as IPF-TA (Tensile Axis) maps.

Prior to deformation, a large EBSD map of the initial state of the samples was performed (BM: 1.0×1.0 mm^2, step size 1.031 µm; weld: 0.103×0.077 mm^2, step size 0.106 µm). During in situ tensile tests, stops were made at different strain levels to record SEM images of the deformed surface, within the initially EBSD mapped area. These stops correspond to the discontinuities in the stress-strain curves of the BM and welded samples (Fig. 3), caused by stress relaxation.

As can be seen on the curve in Fig. 3-a, 8 stops were made every 2% of plastic deformation from $\varepsilon_p = 0.8\%$ to $\varepsilon_p = 14.6\%$ during the BM sample experiment. The final stress drop at 16.6% corresponds to BM sample failure. 150 grains were extracted from the BM initial EBSD map and identified in the subsequent deformed SEM images. Based on the available slip systems in α titanium (Table 1), a Schmid analysis was performed on these grains in an attempt to index the observed slip traces on the SEM images. The Schmid analysis procedure is described in Appendix A.

In the case of the welded sample, three stops were made at strain 0.9%, 2.2% and 4.1% as seen in Fig. 3-b. In addition to SEM images, deformation of the welded sample was also followed with small EBSD maps of specific areas. Finally, the tensile test was stopped before failure in order to record a large EBSD map of the same region of interest as in the initial state. ARPGE software [17] was used to determine the orientation of the former β grains before martensitic transformation in the welded zone.

3. Results

3.1. Base Metal Analysis

Fig. 4-a depicts the tensile axis IPF map of the base metal. One can note a slightly banded microstructure with preferred c-axis orientation either aligned (red grains) or perpendicular (blue/green grains) to the tensile direction. The subset of 150 selected grains within the previous map are represented in the hexagonal standard IPF triangle in Fig. 4-b. They are rather homogeneously distributed in all regions of the triangle. The grain size is illustrated in the color code, with an average of 15–20 µm.

Table 2
Chemical composition of Ti-6Al-4V (B348 grade 5 standard).

Element	Ti	Al	V	C	Fe	O	N	H
% weight	Base	5.5–6.75	3.5–4.5	< 0.08	< 0.40	< 0.20	< 0.05	< 0.015